Journal of Electroceramics 6:1, 21–25, 2001
© 2000 Kluwer Academic Publishers. Printed in The Netherlands.

# $Pb(Mg_{1/3}Nb_{2/3})_{0.97}Ti_{0.03}O_3$ Ferroelectric Thin Films, Deposited by Laser Ablation on TiN Bottom Electrodes*

A. FUNDORA[1,2], E. MARTÍNEZ[1], H. AMORÍN[2,3], O. E. CONTRERAS[1], & J. M. SIQUEIROS[3]

[1]*Posgrado de Física de Materiales, Centro de Investigación Cientifica y de Educación Superior de Ensenada, Ensenada, B. Cfa., México;* [2]*Facultad de Física-IMRE, Universidad de la Habana, Vedado, La Habana 10400, Cuba;* [3]*Centro de Ciencias de la Materia Condensada, Universidad Nacional Autónoma de México, Apartado Postal 2681, Ensenada, Baja California., México.*

Submitted August 25, 1999; Revised March 10, 2000; Accepted June 30, 2000

**Abstract.** $Pb(Mg_{1/3}Nb_{2/3})_{0.97}Ti_{0.03}O_3$ (PMNT) polycrystalline thin films were deposited on Titanium Nitride electrodes at different temperatures by laser ablation, using a wavelength of 248 nm. The morphology of the films was analyzed by scanning electron microscopy (SEM). The nature of the ferroelectric layer-electrode interface is studied by transmission electron microscopy (TEM) as well as the effect of its characteristics in the performance of the multilayer system. The influence of the annealing temperature on the dielectric properties was studied by hysteresis and fatigue measurements.

**Keywords:** ferroelectric thin films, dielectric properties, microstructural properties

## 1. Introduction

$Pb(Mg_{1/3}Nb_{2/3}O_3$ (PMN) is the best known relaxor material. It exhibits a high dielectric constant, high electrostrictive coefficient and diffuse phase transition near $-15°$ C [1,2]. Many efforts have been made to modify the transition temperature toward higher values by using $Pb(Mg_{1/3}Nb_{2/3})O_3$ - $PbTiO_3$ (PMNT) solid-solutions [3]. The ferroelectric properties of PMNT cover a wide range of applications, dependent on the amount of Ti in the solid solution. A large induced electrostrictive strain can be obtained from compositions containing small amounts of Ti and the piezoelectric effect becomes significant near the morphotropic phase boundary, where the Ti content is approximately 35 % [4]. PMN and PMNT thin films have become attractive also for microelectronic applications such as dynamic and ferroelectric random access memory (DRAM, FRAM), and microactuator applications [5].

Pulsed laser deposition (PLD) has been shown to be a good technique to grow ceramic thin films because, under the proper conditions, it is stoichiometry preserving. Being that PMN and PMNT are complex compounds, PLD is a very attractive possibility.

Pt-based metal films are generally used as bottom electrodes, but it is difficult to prepare highly oriented ferroelectric films on such electrodes. On the other hand, the use of oxide substrates is not compatible with Si integrated circuits [6].

In many reports, TiN is used as electrode because of its low resistivity (20–100 $\mu\Omega$cm) and good adhesion to Si and $SiO_2$ substrates [7–9]. In this work, the fabrication, characterization and physical properties of $Pb(Mg_{1/3}Nb_{2/3})_{0.97}Ti_{0.03}O_3$ ferroelectric thin films deposited on TiN electrodes are reported.

## 2. Experimental Procedure

The PMNT/TiN films were grown in a high vacuum chamber with base pressure of the order of $10^{-4}$ Pa and a working oxygen pressure of 26 Pa. The target was fixed in a rotating mount moving at constant angular speed to favor thickness uniformity. A KrF excimer laser (LEXTRA 200 by Lambda Physik) with 248nm wavelength, 30 ns pulse duration, 10 Hz repetition rate and a fluence of 2 J/cm$^2$ was used for deposition. The distance between the target and the

$TiN/SiO_2/Si$ (100) substrate was 100 mm. The resulting films were annealed at 500 (PMNT500) and 600°C (PMNT600). The TiN films were prepared by using reactive sputtering of Ti in a 9 to 1 mixture of argon and nitrogen at a pressure of 0.6 Pa, with substrate temperature of 450°C. The resulting TiN films were polycrystalline. The surface and cross-section morphology of the PMNT films were examined with a JSM-5300 scanning electron microscope by JEOL. Cross-sectional TEM specimens were prepared using the standard ion milling technique. The samples were examined with a JEOL 2010 transmission electron microscope. Selected area diffraction (SAD) and micro-diffraction were used to determine the crystalline phases present. The ferroelectric properties of the PMNT thin films were measured by using a RT-66A ferroelectric tester from Radiant Technologies Inc.

## 3. Results and Discussion

Scanning electron microscopy analysis revealed that the surface of PMNT films deposited by laser ablation presented a regular granular layer, with uniform grain size regardless of the annealing temperature [Fig. 1(a) and 1(b)]. The PMNT target used for film deposition had a relatively high density (95% of the theoretical value), which explains the presence of particulates in the films, characteristic of dense targets. A cross-sectional view of a thin film annealed at 500°C is shown in Fig. 1(c) where a columnar growth is observed. The growth on the $TiN/SiO_2/Si(100)$ metallized surface will depend on the morphology of the electrode, in this case, a clean TiN surface which will strongly influence the growth habit of the PMNT films.

Its known that the PMNT system is a ferroelectric material with diffuse phase transition, which is due to the presence of polar nanodomains above the phase transition temperature [10], produced by compositional inhomogeneities [1,11,12]. In this case, the critical temperature, instead of having a precise value, becomes a distribution around the temperature value for maximum permittivity. In Fig. 2, the hysteresis curves of PMNT thin films, taken above the transition temperature $T_c$ of this material, are shown. These curves are similar to those of ferroelectric PMNT in

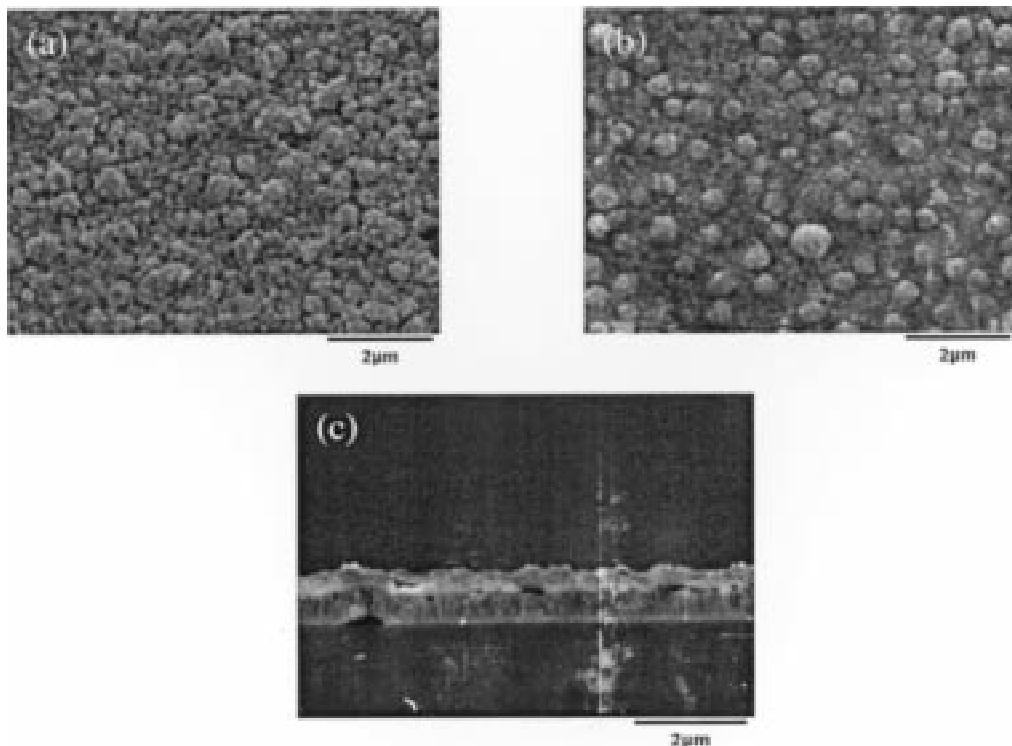


*Fig. 1.* a) SEM micrographs showing the post-annealed surface morphology for PMNT500, b) PMNT600, c) Cross-sectional view of a PMNT thin film annealed at 500°C.

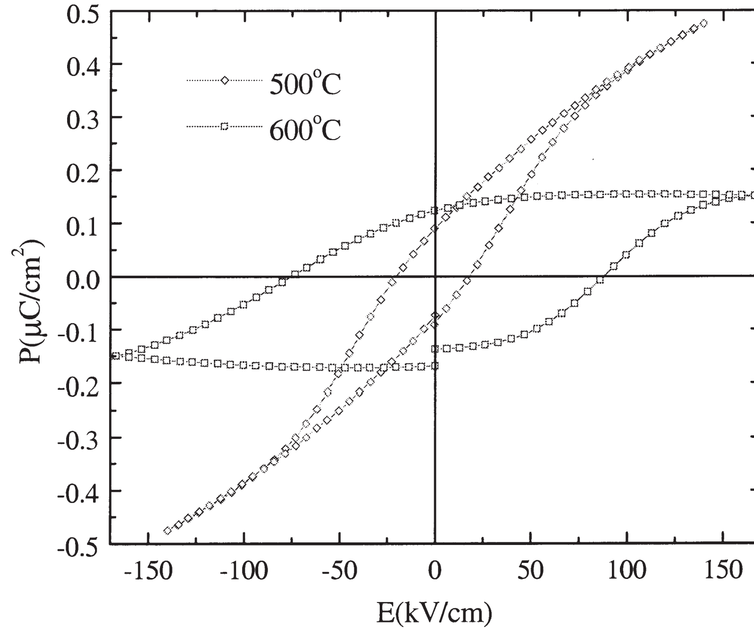


*Fig. 2.* P-E hysteresis curves of PMNT thin films deposited by Pulsed Laser Deposition annealed at 500°C and 600°C with an applied electrical field applied from 20 to 140 KV/cm.

the bulk. It is clearly seen that the PMNT600 film presents higher dielectric losses than the PMNT500 film. Also, retention loss is more noticeable in the PMNT600 sample. The polar nanostructures embedded in a paraelectric matrix of PMNT explaining the hysteretic behavior above $T_c$ are clearly seen in the TEM micrographs shown in Fig. 3 (A). Well-crystallized layers of TiN and PMNT with features of the order of 100 nm and a well-defined interface are shown in Fig. 3 (B).

The discontinuity of the hysteresis loop along the polarization axis for the film annealed at 600°C is considerable larger than for the 500°C film. Following Auciello *et al.* [13], such discontinuity will depend on

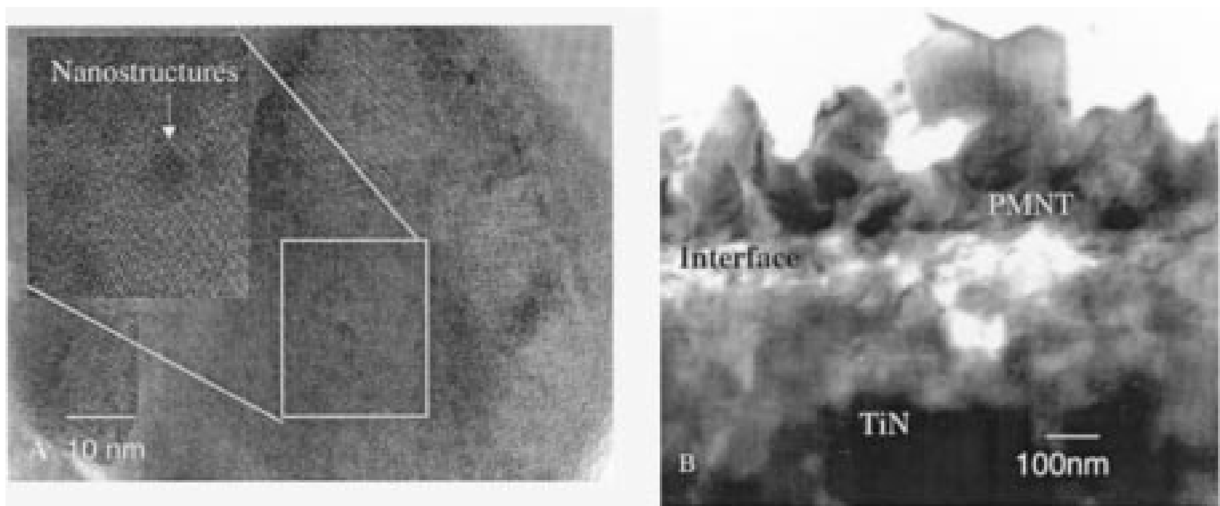


*Fig. 3.* A) HRTEM of a PMN-PT thin film and B) TEM micrograph of the TiN - PMNT interface.

the relaxation of the remanent polarization which in turn depends on the measurement electric pulse. In this case, the delay time was 100 ms, enough to allow strong relaxation and a big discontinuity in the hysteresis loop in a system where the polar response is attributed to nanoparticles in a paraelectric matrix, shown in Figure 3. The difference in the behavior of the PMNT500 films as compared with the PMNT600 films is attributable to the fact that TiN films undergo an oxidizing process when heated above 550 °C [14]. The film will then loose oxygen to form a $TiO_2$ phase creating oxygen vacancies and free charges that will pin the polar domains.

Ferroelectric hysteresis loops of the films annealed at 500 and 600°C showed saturation for an applied electric field over 150 kV/cm. Table 1 shows the values for $P_r$ and $E_c$ for both films. The values for $P_r$ are nearly the same but the value of $E_c$ for the PMNT600 film is much larger than that for the PMNT500 film due to stronger domain pinning. The obtained polarization ($P$) values are lower than those reported on literature for this system [15], because the measurements were performed above the nominal critical temperature of the ferroelectric material.

Fig. 4 represents the fatigue characteristics of the ferroelectric PMNT/TiN film post-annealed at 600°C at 5 V with 1 kHz, bipolar pulses. In this figure, at about $10^3$ cycles, a degradation in the values of $P^*$ and $P^\wedge$ can be observed. No perfect symmetry between positive and negative $P^*$ and $P^\wedge$ values is to be expected due to the asymmetric processes taking place at the upper and bottom electrodes. These results could indicate that the fields created by space-charge accumulation within the films, at specific defect sites, are becoming distributed throughout the film as the number of polarization reversals increases [19]. This effect would result in the reduction to zero of the relaxed remanent polarization via domain switching.

Fig. 3 shows that the films grow in polycrystalline form where a clear difference between the grain and the grain boundary is seen; charge trapping is then to be expected causing domain pinning. [16]

*Table 1.* Value of $P_r$ and $E_c$ of PMNT thin films, annealing of 500 and 600°C respectively.

| Sample | $P_r$ ($\mu$C/cm$^2$) | $E_c$ (kV/cm) |
|---|---|---|
| PMNT 500 | 0.08 | 17 |
| PMNT 600 | 0.12 | 87 |

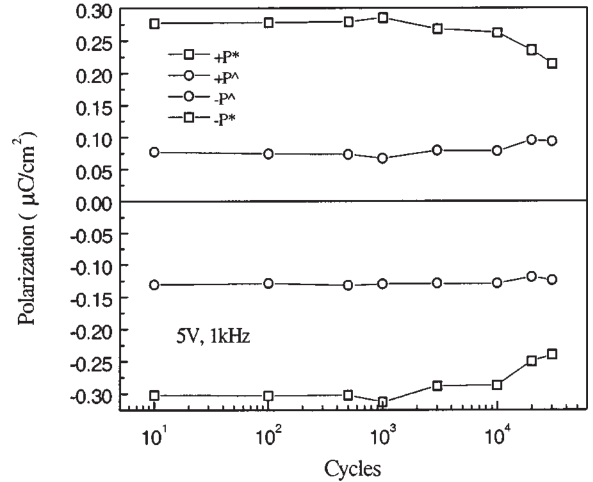


*Fig. 4.* Polarization fatigue performance of the PMNT thin films annealed at 600°C.

Fig. 5 (a) shows the initial *P-E* loop of the PMNT/TiN thin films annealed at 600°C. The hysteresis loop shown in Figure 5(b) was taken after subjecting the capacitor to ~$10^3$ field reversal cycles. The switchable polarization has been significantly suppressed by field cycling, as observed by many other researchers [17,20–25]. The sample shows a different hysteretic behavior after fatigue measurements, meaning lower coercive field and dielectric loses and higher saturation polarization. This result is consistent with the fatigue data show in Fig. 4.

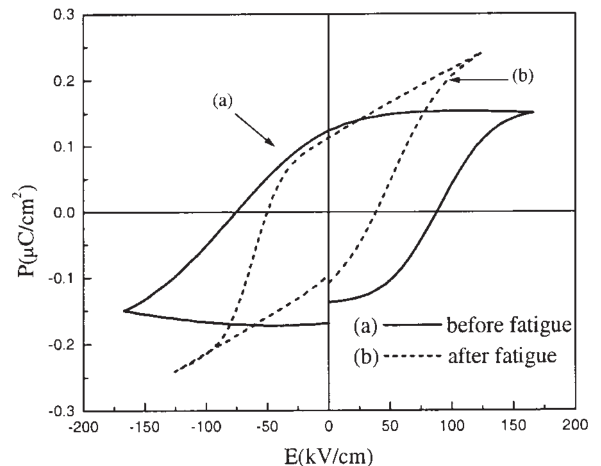


*Fig. 5.* Show the hysteresis loops of the PMNT/TiN thin films annealed at 600°C, before and after fatigue measurements.

## 4. Conclusion

To the authors' knowledge, this is the first report of ferroelectric $Pb(Mg_{1/3}Nb_{2/3})_{0.97}Ti_{0.03}O_3$ thin films grown by pulsed laser deposition on TiN bottom electrode. The films were uniform, well adhered and with low crystallinity as deposited. The resulting films were heat treated at 500 and 600°C rendering well-crystallized films with no residual amorphous phases, as shown by SEM and TEM. A better ferroelectric performance is observed in the PMNT500 films indicating a negative influence of the TiN electrode at higher temperatures probably due to an oxidizing process. Hysteresis was observed above the nominal transition temperature of PMNT suggesting a ferroelectric behavior with diffuse phase transition. Fatigue of the ferroelectric properties was observed beyond $10^6$ cycles.


## Acknowledgments

This work was partially sponsored by CoNaCyT Proj. No. 26314E, DGAPA Proj. No. IN104000. We thank, I.Gradilla, F. Ruiz, E. Aparicio, A. Tiznado and E. Medina for their technical help. A. Fundora thanks the Foreign Ministry of México for their support. H. Amorín, thanks CLAF, Rio de Janeiro-Brazil for financial support.


## References


1. G.A. Smolensky, *J. Physical Soc. of Japan,* **28,** 26 (1970).
2. S.L. Swartz, T.R. Shrout, W.A. Schultze, and L.E. Cross, *J. Amer. Ceram. Soc.,* **67,** 311 (1984).
3. T.R. Shrout and J. Fielding, *Ultrasonic Symposium,* 711 (1990).
4. S.W. Choi, T.R. Shrout, S.J. Jang and A.S. Bhalla, *Ferroelectrics,* **29,** 100 (1989).
5. P.K. Larsen, R. Cuppens, and G.A.C.M. Spiering, *Ferroelectrics,* **128,** 265 (1992).
6. M.J. Shyu, T.J. Hong, T.J. Yang, and T.B. Wu, *Jpn. J. Appl. Phys.,* **34**(7A), (1995).
7. W. Wang, J.H. Booske, H.L. Liu, S.S. Gearhart, and J.L. Shohet, *J. Mater. Res.,* **13**(3), (1998).
8. K. Holloway, P.M. Fryer, C. Cabral, Jr., J.M.E. Harper, P.J. Bailey, and K.H. Kellerher, *J. Apply. Phys.,* **71,** 543 (1992).
9. N. Mattoso, C. Achete, and F.L. Freire, *Thin Solid Films,* **220,** 184 (1992).
10. A. Fundora, A. Vázquez, J. Portelles, F. Calderón, J.M. Siqueiros, *J. Non-Cryst. Sol.,* **235,** 567 (1998).
11. X. Dai, Z. Xu, D. Viehland, *J. Appl. Phys.,* **79**(2), 1021 (1995).
12. L.E. Cross, *Ferroelectrics,* **76,** 241 (1987).
13. O. Auciello, L. Mantese, J. Duarte, X. Chen, S.H. Rou, A.I. Kingon, A.F. Schreiner, and A.R. Krauss, *J. Appl. Phys.,* **73**(10), 5197 (1993).
14. M. Wittmer, J. Noser, and H. Melchior, *J. Appl. Phys.,* 52(11), 6659 (1981).
15. J-P Maria, W. Hackenberger, and S. Trolier-MacKinstry, *J. Appl Phys.,* **84**(9), 1998.
16. W.L. Warren, D. Dimos, B.A. Tuttle, G.E. Pike, R.W. Schwartz, and P.J. Clews, *J. Appl. Phys.,* **77**(12), 6695 (1995).
17. Seshu B. Desu, in K. Yoo, *Integrated Ferroelectrics.,* **3,** 365 (1993).
18. I.K. Yoo and S.B. Desu, *J. Mat's. Sci. and Eng.,* **B 13,** 319 (1992).
19. I.K. Yoo and S.B. Desu, *MRS Proc.,* **243,** 323, 329 (1992).
20. I.K. Yoo and S.B. Desu, *Phys. Status Solidi,* **A133,** 565 (1992).
21. T.S. Kim, D.J. Kim, J.K. Lee, and H.J. Jung, *J. Mater. Res.,* **13**(12) (1998).
22. K. Yoo, S.B. Desu, and J. Xing, *MRS Symp. Proc.,* **310,** 165 (1993).
23. A.I. Kingon, O. Auciello, M.S. Ameen, S.H. Rou, and A.R. Kraus, *Appl. Phys. Lett.,* **55,** 301 (1989).
24. W.Y. Pan, C.F. Yan, and B.A. Tuttle, *Ceram. Trans.,* **25,** 385 (1992).
25. O.Y. Jiang, E.C. Subbarao, and L.E. Cross, *J. Appl. Phys.,* **75,** 7433, (1994).